Free-running Model Tests of a Damaged Ship in Head and Following Seas

Taegu, Lim, *Korea Research Institute of Ships and Ocean Engineering* ltg88@kriso.re.kr

Jeonghwa, Seo, *Seoul National University* thamjang@snu.ac.kr

Sung Taek, Park, *Seoul National University* probpst@snu.ac.kr

Shin Hyung, Rhee, *Seoul National University* shr@snu.ac.kr

ABSTRACT

A series of tests using a course-keeping model ship in a towing tank were carried out for research on Safe Return to Port (SRtP). A passenger ship model with a damaged compartment was modified to be equipped with propellers and rudders for a course-keeping maneuver by an onboard autopilot system. The 6DoF motion of the test model was measured by a wireless inertial measurement unit (IMU) and gyro sensors to achieve fully wireless model tests. Advance speed and motion response in various wave conditions were measured and analyzed to investigate the propulsion and maneuvering performances of the damaged ship model in head and following seas.

Keywords: *Free-running test, Safe Return to Port, Damaged ship stability*

1. INTRODUCTION

Recently the scale of damages in maritime accidents has grown with the increasing sizes of vessels. In the case of passenger ship accidents especially, a great number of casualties often results; thus, efforts to improve regulations and vessel designs to prevent casualties are required. The International Maritime Organization (IMO) effected a regulation on the Safe Return to Port (SRtP) of a passenger ship with a length over 120 m in July 2010 (Spanos and Papanikolaou, 2012).

SRtP regulations require the survivability of vessels after fire or flooding under a casualty threshold. After an accident occurs, the vessel must be able to return to a port nearby without external help. It also refers to the minimum requirements of the propulsion performance and maneuverability of the vessel in certain weather conditions; thus, assessing the stability and maneuverability of the vessel under various weather conditions is needed during the stage of designing the ship to judge whether the vessel follows SRtP regulations.

Traditionally ship stability was analyzed by model tests and analytic methods based on the potential flow theory. Analytic methods have been widely used, as they have the merits of high reliability and low computational resource requirements. For cases of unconventional hull geometry and nonlinear phenomena, however, applying analytic methods with the potential flow theory has limitations, and modifications to the methods are necessary.

Parametric roll and broaching are well-known nonlinear physical phenomena in ship stability. Model tests on those nonlinear vessel motions have been performed, and analytic methods are suggested (Bulian, 2005; Lee et al., 2007; Neves and Rodriguez, 2007).

To achieve an analysis of the nonlinear phenomena, an analysis of the fluid dynamics should precede, i.e., eddy-making, turbulent boundary layer, and viscous roll damping. These features are caused by the viscous nature of fluids; thus, approaching the analysis in consideration of the viscosity of fluid is in high demand and computational fluid dynamics (CFD) is the only viable method to treat the viscous flow field. In these days, CFD techniques have been applied to various fields of naval hydrodynamics: the self-propulsion performance of vessel (Seo et al., 2010; Carrica et al., 2011), the motions in waves (Carrica et al., 2007; Simonsen et al., 2013), and the prediction of maneuverability (Araki et al., 2012; Carrica et al., 2013). Approaches with CFD have produced good results, especially on the roll motion of vessels highly affected by the viscosity of fluid (Wilson et al., 2006). As roll motion is the most important criteria for judging the stability of a ship, it is obvious the CFD analysis will substitute traditional analytic methods based on the potential flow theory.

A CFD analysis also has been introduced to assess the issue of damaged ship stability. In the case of damaged ship stability, the interaction between flooded water and ship motion causes highly nonlinear phenomena (Gao et al., 2011). As damaged ship stability is one of the most important elements of SRtP conditions, approaches with CFD are expected to be essential during the design stage of passenger ships under SRtP regulation.

Before applying the CFD method to practical cases, it should be validated through existing experimental results. In the design of experiments for a validation database for CFD, the existence of nonlinear phenomena should be considered, as CFD approaches aim to predict the nonlinear motion of a vessel.

For experimental study on nonlinear motion of vessel, the motion response of a moored model in various waves was measured, and the parametric roll behavior was identified through a series of model tests (Begovic et al., 2013; Lee et al., 2012). Also, a gradual increase in the roll motion of a moored model in head seas has been reported and provided for the CFD validation database (Lim et al., 2014). In these tests, however, the restrained motion of the test model was measured, as the model was in a stationary condition with a mooring system.

To predict the stability of practical vessels with high fidelity, tests with a free-running model are required, as it does not require an external towing force. The free-running model has been used to test the seakeeping ability and maneuverability of vessels, but an intact model was used for most tests (Yoon et al., 2007; Sadat-Hosseini et al., 2010; Sadat-Hosseini et al., 2011). For the provision of a CFD validation database, free-running tests in waves must be achieved in damaged condition, and the results should be compared with those achieved in intact condition. Finally, the validated CFD methods can be applied to examine damaged ship stability problems.

In the present study, a free-running model of a passenger ship was used to carry out motion measurements in waves. Tests were designed by SRtP regulations, and the effects of wave conditions and flooded water behaviors on the motion of the test model were investigated.

2. EXPERIMENTAL METHODS

2.1 Test facility

Tests were carried out in the Seoul National University towing tank, the length, width, and depth of which are 110 m, 8 m, and 3.5 m, respectively. Figure 1 shows a schematic diagram of the towing tank, including the eight plunger-type wave makers located at the end of the towing tank. The initial locations of the test model in head seas and following seas were at 50 m and 20 m from the wave maker, respectively.

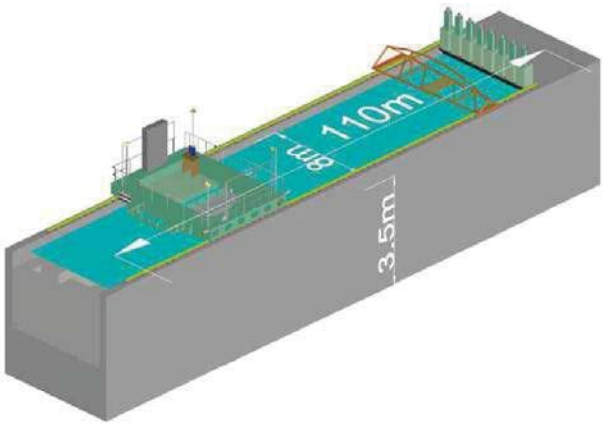

Figure 1 Schematic diagram of the Seoul National University towing tank.

2.2 Test model

A passenger ship hull designed by the Ship Stability Research Centre (SSRC) was used for the test model. It has a bulbous bow and a skeg on the stern. This hull was used for the study on damaged ship stability with a mooring system. Figure 2 shows the design of the test model.

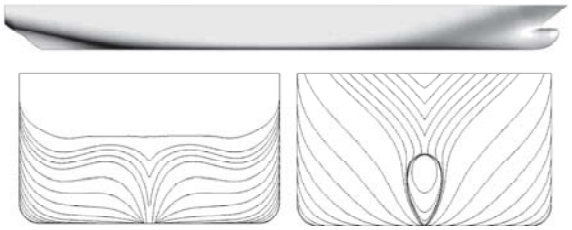

Figure 2 Lines and profile of the test model.

Following the test procedures and recommendations of the seakeeping tests presented by the International Towing Tank Conference (ITTC), the size of the towing tank limited the size of the model ship. The scale ratio of the model was 1/82.57, and the length of the model was 3 m. The principal particulars of the SSRC passenger ship are presented in Table 1. Arrays of studs were attached at station 19 and the bulbous bow to stimulate turbulent flow. Figure 3 shows the constructed test model.

Table 1 Principal particulars of the SSRC passenger ship and test model.

Item	Full Scale	Model Ship
Scale Ratio	1	1/82.57
Length between Perpendiculars (m)	247.7	3
Beam (m)	35.5	0.43
Draft (m)	8.3	0.1
Displacement (m^3)	56514.5	0.312
Propeller Diameter (m)	6	0.073
LCG from amidships (m)	-6.329	-0.077
KB (m)	4.085	0.049
KM (m)	18.781	0.227
KG (m)	16.393	0.199
GM (m)	2.388	0.029
k_{xx}	14.814	0.179
k_{yy}	61.925	0.750

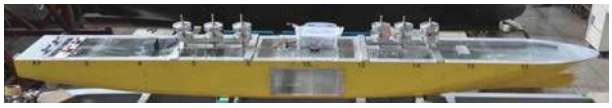

Figure 3 Test model.

A damaged compartment was installed amidships to represent the damaged condition. The location and design of the damaged compartment was identical to the experiments of Lee et al. (2012). Figure 4 shows the design and dimensions of the damaged compartment.

It consisted of two compartments: a damaged compartment located astern (Compartment 1) had an opening to the outside, and a damaged compartment located fore (Compartment 2) had only a connection with Compartment 1. The connection was on the free surface; thus, flooding to Compartment 2 was not expected in a static condition without severe motion. Every compartment had a ventilation hole to minimize the effects of air compression on the flooding behavior. If flooding to Compartment

1 occurred, the model ship gained 5.82 kg of flooded water and an initial heel angle of 2.83°.

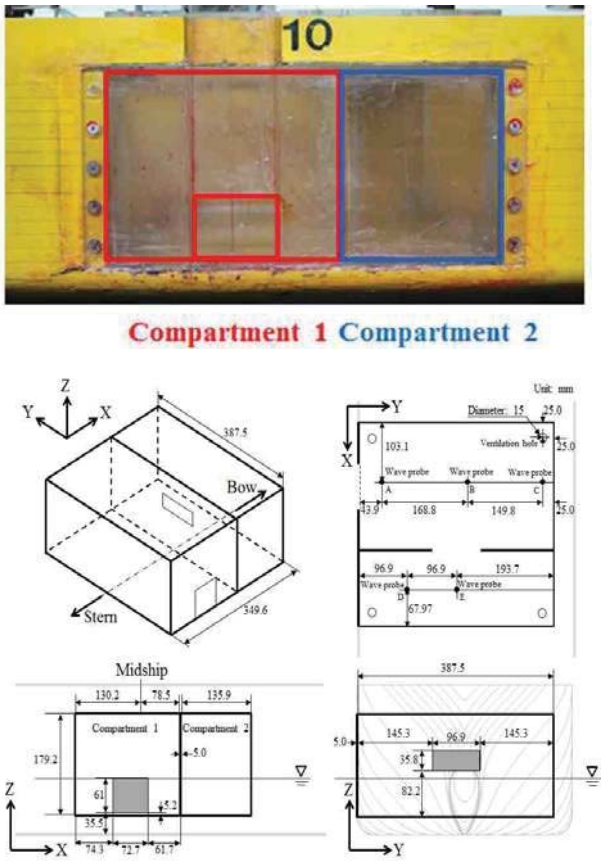

Figure 4 Geometry of the damaged compartment.

2.3 Autopilot system

Two propellers and rudders were appended on the test model to enable maneuverability. The design of a six-blade propeller in the present study was a modified design of the KP505 propeller, of which the design has been open (Paik et al., 2004; Seo et al., 2010). Its pitch ratio at 0.7 R was 0.997. Propeller shafts were supported by L-type struts, which were connected to the center skeg and stern. The profile of the rudder was NACA0012 hydrofoil. Figure 5 shows the fully appended stern of the test model.

Figure 5 Fully appended stern of the test model.

The autopilot system controlled the rudder angle and propeller revolution rate. The heading angle of the test model was measured by a gyro sensor, and the rudder angle was varied by a P controller, the parameter of which was 1.5. The propeller revolution rate was controlled by a PD controller, and the parameters of the P and D controllers were 20 and 8, respectively.

The motion of the model was measured by gyro sensors on the autopilot system and a wireless inertial measurement unit (IMU). Two measurement systems worked independently. The repetition rate of the wireless IMU was 100 Hz. The autopilot system transmitted motion and control signals to a laptop with a repetition rate of 16 Hz.

2.4 Test conditions

Based on the SRtP regulation suggested by Germanischer Lloyd (GL, 2009), the wave and propeller conditions were chosen. In the SRtP regulation, a vessel should achieve an advance speed of 7 knots or half of the design speed in normal weather conditions. In addition, the vessel should preserve maneuverability in unfavorable weather conditions. Normal and unfavorable weather conditions correspond to Sea states 5 and 6, respectively. Table 2 describes the wave conditions for the present SRtP tests.

Table 2 Wave conditions for SRtP tests.

		Normal weather conditions		Unfavorable weather conditions	
		Full scale	Model scale	Full scale	Model scale
Period (s)	T	6.7	0.737	8.3	0.913
Wave number (rad/m)	k	0.090	7.415	0.059	4.832
Wave length (m)	λ	69.9	0.847	107	1.300
Wave Amplitude (m)	A	2.8	0.034	5.4	0.066

To determine the minimum propulsion power, the propeller revolution rate at an advance speed that corresponds to 7 knots in the full scale (0.396 m/s) was investigated in calm water tests. It was 595 rpm, and the propeller revolution rate for tests was fixed at 615 rpm, considering the powering margin in the waves.

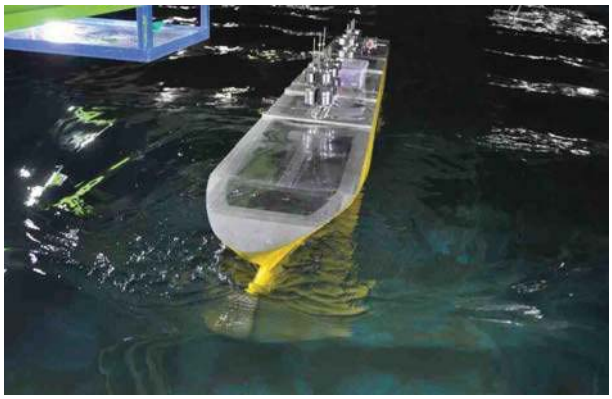

Figure 6 Snapshot of the free-running test.

Tests were performed in head and following seas conditions. The model was released in a stationary condition, and the motion in the time range with a converged speed was sampled and analyzed. Figure 6 shows the snapshot of the model test in head seas.

3. RESULTS AND DISCUSSIONS

3.1 Pitching motion

Figures 7 and 8 show the time history of the pitching motion of the test model. In normal weather conditions, the motion response in following seas was greater than that in head seas, while the pitching motion in head seas increased in unfavorable weather conditions.

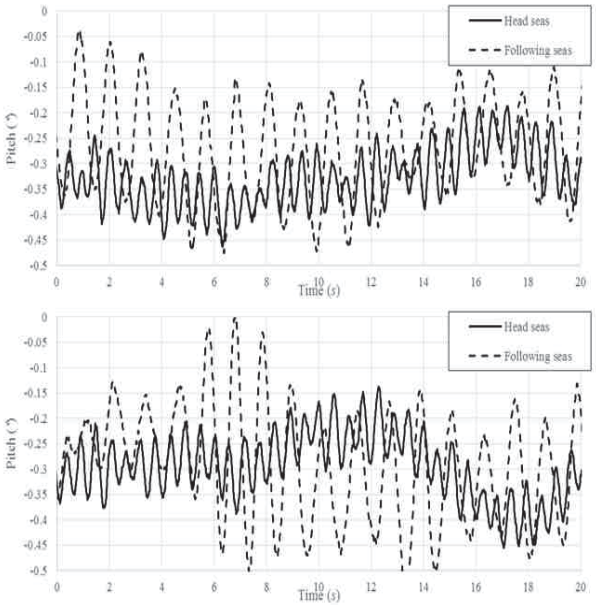

Figure 7 Time history of the pitching motion in normal weather conditions (top: intact condition; bottom: damaged condition).

When the pitching motion of a ship in waves occurs, the bow and stern of the ship move vertically in the water, resulting in slamming. Tendency of slamming, however, showed difference in cases of the bow and stern. As the bulbous bow and the bow flare was immersed, slamming occurred in all wave conditions. Slamming on the stern with flat transom, in contrast to the bow slamming, made high impact over certain wave height condition; thus, slamming on the stern restrained pitching motion in unfavorable weather condition only. In normal weather condition, slamming on the bow was dominant and pitching motion in head seas was smaller than that in following seas.

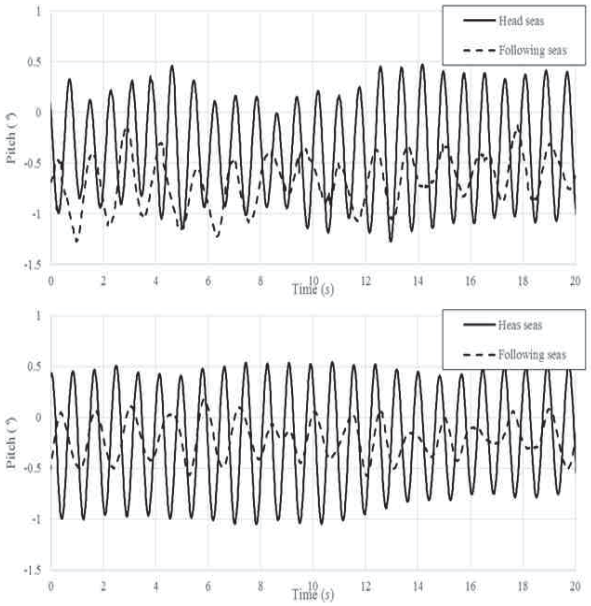

Figure 8 Time history of the pitching motion in unfavorable weather conditions (top: intact condition; bottom: damaged condition).

In all cases, the magnitude and period of the pitching motion in following seas was less regular than in head seas. In following seas, the incoming wave was disturbed by the Kelvin wave and propeller wake and could not maintain its waveform strictly.

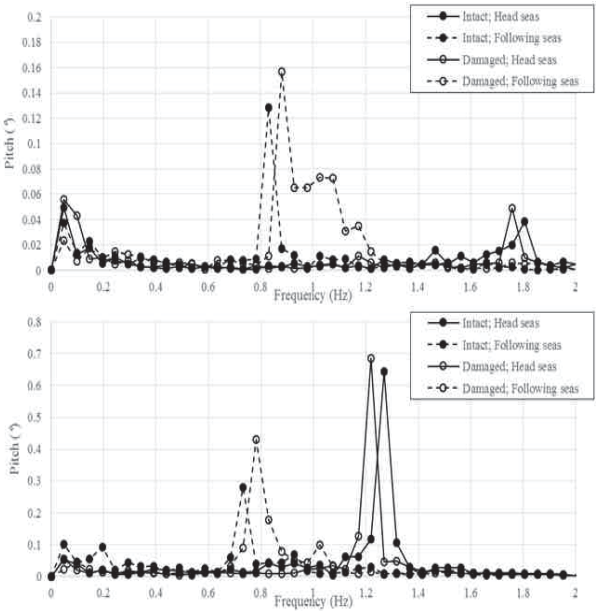

Figure 9 FFT analysis results of the pitching motion (top: normal weather conditions; bottom: unfavorable weather conditions).

Figure 9 shows the results of a fast Fourier transform (FFT) analysis of the pitching motion. The dominant frequency and magnitude of the pitching motion were identified. As stated above, the dominant frequency was clearer in head seas than in following seas due to clear waveform of incoming wave. Also, the magnitude of the pitching motion in damaged condition was greater, as the flooded water led to a loss of stability.

3.2 Speed measurement

The dominant frequency from the FFT analysis was identical to the wave encounter frequency, as the pitching motion was directly induced by waves. Using the incoming and encounter wave frequencies, the advance speed of the model could be derived by the Doppler effect. The derived advance speed of the intact free-running model is presented in Table 3.

Table 3 Advance speed of the intact model ship.

Wave condition		Wave encounter frequency (rad/s)	Advance speed (m/s)
Calm water		-	0.419
Normal weather condition (ω_0 = 8.52 rad/s)	Head seas	11.29	0.382
	Following seas	5.219	0.446
Unfavorable weather condition (ω_0 = 6.88 rad/s)	Head seas	7.933	0.227
	Following seas	4.699	0.471

Advance speed decreased significantly in head seas, while a small increase was observed in following seas because of the difference in the relative velocity of the waves. In head seas condition, the ship and waves were in the opposite direction; thus, the relative velocity of the incoming wave and test model increased,

resulting in large added resistance. As the group velocity of the wave was greater than the advance speed in following seas condition, the ship gained an additional propulsive force from the waves and the advance speed in following seas exceeds that in calm water.

Advance speed results in damaged condition are presented in Table 4. The flooding behavior that caused eddy-making and violent free surface in the damaged compartment was expected to create additional resistance, and a decrease in advance speed was observed in every wave condition. Retardation of the advance speed was more significant in unfavorable weather conditions, as strong flooding behavior occurred through the damaged hole.

Table 4 Advance speed of the damaged model ship.

Wave condition		Wave encounter frequency (rad/s)	Advance speed (m/s)
Calm water		-	0.410
Normal weather condition (ω_0 = 8.52 rad/s)	Head seas	11.12	0.340
	Following seas	5.322	0.404
Unfavorable weather condition (ω_0 = 6.88 rad/s)	Head seas	7.634	0.163
	Following seas	4.865	0.408

3.3 Roll motion

The flooding behavior in the damaged compartment induced roll motion, as well as the retardation of advance speed. Figures 10 and 11 shows the time history of the roll motion in normal weather conditions.

Roll motion was not expected in the ideal case when heading angle was perfectly aligned with wave direction. In the experiments, however, asymmetric flow field developed as the flow around the test model was not exactly symmetric, due to the slight yaw motion during autopilot course-keeping maneuver. Even small asymmetry caused coupled roll and pitching motion in head and following seas condition, and the roll motion period was expected to be identical to the wave encounter period.

In following seas condition, roll motion was regular and its period was identical to the wave encounter period. In normal weather condition, however, the roll motion period was identical to the natural roll period of the test model, although pitching motion period was identical to the wave encounter period. That implied existence of resonance of roll motion only. In the damaged condition, the resonance motion was interfered with by the flooded water; thus, the roll motion was not fully developed and irregular motion was observed.

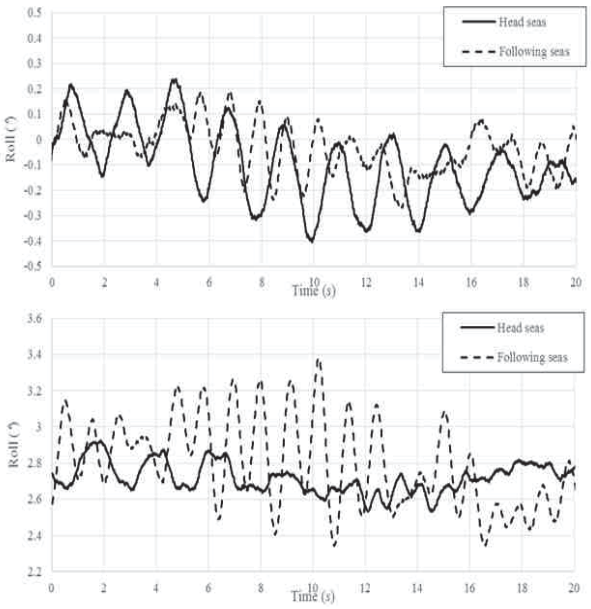

Figure 10 Time history of the roll motion in normal weather conditions (top: intact condition; bottom: damaged condition).

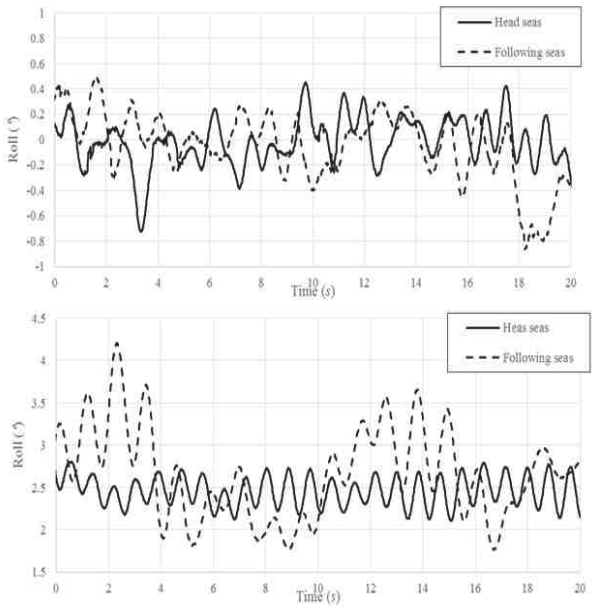

Figure 11 Time history of roll motion in unfavorable weather conditions (top: intact condition; bottom: damaged condition).

Figure 11 shows the time history of roll motion in unfavorable weather conditions. Strong flooding behaviors appear in unfavorable weather conditions; thus, roll motion was induced in damaged condition and its period was identical to the wave encounter period. In intact case, however, roll motion in head seas was irregular and the resonance motion in the natural roll period of the model was not observed, as there was no excitation force of the roll motion.

4. CONCLUSIONS

In the present study, a free-running model ship was constructed to perform experimental research on the SRtP of a damaged ship. Motion responses of the damaged ship model in head and following seas were measured, and the influences of the damaged compartment and wave conditions on the motion responses of the model were identified.

In the course-keeping tests in head and following seas, the characteristics of pitching motion were analyzed first. Slamming on the stern suppressed the pitching motion of the test model in unfavorable weather conditions; therefore, the pitching motion responses in following seas was less than those in head seas in unfavorable weather conditions.

The advance speed of the model was derived from the wave encounter frequency. In head seas, incoming waves generated additional resistance on the hull and caused the advance speed to decrease severely. In following seas, the phase velocity of the waves was faster than the advance speed of the free-running model; thus, the wave increased the advance speed slightly.

In damaged condition, the flooding behavior in the damaged compartment augmented resistance of the ship, resulting in a lower advance speed than in intact condition. In unfavorable weather conditions, retardation of the advance speed was 13% in following seas and 28% in head seas.

The roll motion responses of the ship in waves were also analyzed. The resonance of the roll motion in the natural roll period of the model was observed in intact and normal weather conditions. In damaged condition, however, the periodic flooding behavior stimulated roll motion, and the distinguishable roll period was identical to the wave encounter period.

Through free-running tests, the characteristics of the motion responses of a damaged ship model under SRtP regulations were identified. As future studies, a wireless measurement system for propulsion performance and wave heights in the damaged compartment will be installed on the free-running system to achieve the provision of a reliable validation database for CFD.

5. ACKNOWLEDMENTS

The present study is supported by the Office of Naval Research (ONR) under the supervision of Dr. Ki-Han Kim, the National Research

Foundation of Korea (Grant No. 2013R1A1A2012597), and the Multi-Phenomena CFD Research Center (Grant No. 20090093103), funded by the Ministry of Education, Science and Technology of the Korea Government.

6. REFERENCES

Araki, M., Sadat-Hosseini, H., Sanada, Y., Tanimoto, K., Umeda, N., and Stern, F., 2012, "Estimating Maneuvering Coefficients Using System Identification Methods with Experimental, System-based, and CFD Free-running Trial Data", Ocean Engineering, Vol. 51, pp. 63-84.

Ayaz, Z., Vassalos, D., and Spyrou, K. J., 2006, "Manoeuvring Behaviour of Ships in Extreme Astern Seas", Ocean Engineering, Vol. 33, pp. 2381-2434.

Begovic, E., Mortola, G., Incecik, A., and Day, A. H., 2013, "Experimental Assessment of Intact and Damaged Ship Motions in Head, Beam and Quartering Seas", Ocean Engineering, Vol. 72, pp. 209-226.

Bulian, G., 2005, "Nonlinear Parametric Rolling in Regular Waves-a General Procedure for the Analytical Approximation of the GZ Curve and Its Use in Time Domain Simulations", Ocean Engineering, Vol. 32, pp. 309-330.

Carrica, P. M., Wilson, R. V., Noack, R. W., and Stern, F., 2007, "Ship Motions Using Single-phase Level Set with Dynamic Overset Grids", Computers & Fluids, Vol. 36, pp. 1415-1433.

Carrica, P. M., Huiping, F., and Stern, F., 2011, "Computations of Self-propulsion Free to Sink and Trim and of Motions in Head Waves of the KRISO Container Ship (KCS) Model", Applied Ocean Research, Vol. 33, pp. 309-320.

Carrica, P. M., Ismail, F., Hyman, M., Bhushan, S., and Stern, F., 2013, "Turn and Zigzag maneuvers of a Surface Combatant Using a URANS Approach with Dynamic Overset Grids", Journal of Marine Science and Technology, Vol. 18, pp. 166-181.

Choi, J.E., Min, K.-S., Kim, J. H., Lee, S.B., and Seo, H. W., 2010, "Resistance and Propulsion Characteristics of Various Commercial Ships Based on CFD Results", Ocean Engineering, Vol. 37, pp. 549-566.

Gao, Z., Gao, Q., and Vassalos, D., 2011, "Numerical Simulation of Flooding of a Damaged Ship", Ocean Engineering, Vol. 38, pp. 1649-1662.

Germanischer Lloyd (GL), 2009, "Preliminary Guidelines of Safe Return to Port Capability of Passenger Ships", GL Rules for Classification and Construction, VI-11-02.

International Towing Tank Conference (ITTC), 2011, "Seakeeping Experiments", ITTC-Recommended Procedures and Guidelines, 7.5-02-07-02.1.

Lee, D., Hong, S. Y., and Lee, G.-J., 2007, "Theoretical and Experimental Study on Dynamic Behavior of a Damaged Ship in Waves", Ocean Engineering, Vol. 34, pp. 21-31.

Lee, S., You, J.-M., Lee, H.-H., Lim, T., Rhee, S. H., and Rhee, K.-P., 2012, "Preliminary Tests of a Damaged Ship for CFD Validation", International Journal of Naval Architecture and Ocean Engineering, Vol. 4, pp. 172-181.

Lim, T., Seo, J., Park, S. T., Rhee, S. H., 2014, "Experimental Study on the Safe-Return-to-Port of a Damaged Ship in Head Seas", Proceedings of 30th Symposium on Naval Hydrodynamics, Hobart, Australia.

Neves, M. A. S. and Rodriguez, C. A., 2007,

"Influence of Non-linearities on the Limits of Stability of Ships Rolling in Head Seas", Ocean Engineering, Vol. 34, pp. 1618-1630.

Paik, B. G., Lee, C. M., and Lee, S. J., 2004, "PIV Analysis of Flow around a Container Ship Model with a Rotating Propeller", Experiments in Fluids, Vol. 36, pp. 833-846.

Sadat-Hosseini, H., Stern, F., Olivieri, A., Campana, E., Hashimoto, H., Umeda, N., Bulian, G., and Francescutto, A., 2010, "Head-wave Parametric Rolling of a Surface Combatant", Ocean Engineering, Vol. 37. pp. 859-878.

Sadat-Hosseini, H., Carrica, P., Stern, F., Umeda, N., Hashimoto, H., Yamamura, S., and Mastuda, A., 2011, "CFD, System-based and EFD Study of Ship Dynamic Instability Events: Surf-riding, Periodic Motion, and Broaching", Ocean Engineering, Vol. 38, pp. 88-110.

Seo, J. H., Seol, D. M., Lee, J. H., and Rhee, S. H., 2010, "Flexible CFD Meshing Strategy for Prediction of Ship Resistance and Propulsion Performance", International Journal of Naval Architecture and Ocean Engineering, Vol. 2, pp. 139-145.

Simonsen, C. D., Otzen, J. F., Joncquez, S., and Stern, F., 2013, "EFD and CFD for KCS Heaving and Pitching In Regular Head Waves", Journal of Marine Science and Technology, Vol.18, pp. 435-459.

Spanos, D. A. and Papanikolaou, A. D., 2012, "On the Time Dependence of Survivability of ROPAX Ships", Journal of Marine Science and Technology, Vol. 17, pp. 40-46.

Wilson, R. V., Carrica, P. M., and Stern, F., 2006, "Unsteady RANS Method for Ship Motions with Application to Roll for a Surface Combatant", Computers & Fluids, Vol. 35, pp. 501-524.

Yoon, H. K., Son, N. S., and Lee, G. J., 2007, "Estimation of the Roll Hydrodynamic Moment Model of a Ship by Using the System Identification Method and the Free Running Model Test", IEEE Journal of Oceanic Engineering, Vol. 32, pp. 798-806.